Morphology and Thermal Properties of Fully Syndiotactic Polypropylene

Andrew J. Lovinger,[*,†] **Bernard Lotz,**[‡] **Don D. Davis,**[†] **and Martina Schumacher**[‡]

AT&T Bell Laboratories, Murray Hill, New Jersey 07974, and Institut Charles Sadron (CNRS-ULP), 6 rue Boussingault, 67083 Strasbourg, France

Received May 9, 1994[⊗]

ABSTRACT: The morphology of syndiotactic polypropylene (sPP) containing >99% racemic diads has been investigated following controlled crystallization from the melt in thin films. At high growth temperatures, large rectangular single crystals are obtained with preferred growth along the crystallographic *b*-axis, while at lower temperatures these branch out to yield dendritic, axialitic, and eventually spherulitic aggregates. These crystals exhibit two very unusual properties: transverse fractures and ripples. Both are quasi-periodic, the fractures with a spacing of 3–7 μm and the ripples generally 1 μm or less. The fractures are ubiquitous in samples crystallized both at low and high undercooling and are expected to have severe negative consequences on the mechanical properties and uses of syndiotactic polypropylene. We associate formation of these transverse cracks with an approximate order-of-magnitude greater thermal expansion (and contraction) along the crystallographic *b*-axis *vs* the *a*-axis, which we have documented using variable-temperature X-ray diffractometry. This technique also demonstrated that samples quickly cooled to ambient undergo a heating-induced crystallographic transformation to the fully antichiral packing (cell III) that begins at *ca.* 40 °C below the melting point. Using surface decoration with evaporated polyethylene, we found that the (200) sectors have much more uniform amorphous-surface structure than the (020) sectors and that their folding is oriented along the preferred crystal-growth direction (*b*-axis).

Introduction

Our understanding of the structure of the dominant form of syndiotactic polypropylene (sPP) has undergone drastic revision in the last few years. This form has been known from the early work of Natta and Corradini[1,2] to possess a helical $(t_2g_2)_2$ conformation with a molecular repeat of 0.74 nm. The packing of the chains was considered for over 25 years to be isochiral in a C-centered orthorhombic unit cell (cell I),[1,2] as seen in Figure 1a. However, a few years ago we proposed a different packing that is antichiral at least along the *a*-axis of the unit cell (cell II, Figure 1b), as well as a fully antichiral packing along both *a*- and *b*-axes (cell III, Figure 1c), the latter prevailing at high crystallization or annealing temperatures.[3] All these structural proposals had been obtained from samples of fairly low syndiotacticity (<80% racemic triads).[4]

With the advent of metallocene polymerization,[5] we began structural investigations of essentially fully syndioregular (>99%) polypropylene. We found that the doubled cell III is the stable and dominant form under conditions of slow, controlled crystallization.[6] At lower crystallization temperatures, faster growth rates cause introduction of packing defects, which involve *b*/4 vacancies along the crystal growth direction (*b*-axis) and which were discovered as a result of their accompanying streaking of the *h*20 layer of the reciprocal lattice in electron diffraction[6]. We have recently modeled this streaking and discussed in detail the types of disorder causing it at low and high crystallization temperatures;[6] similar detailed modeling has also been conducted by Auriemma *et al.*[7]

Many laboratories[7–13] have now confirmed the validity and general applicability of our antichirally packed models (cells II and III). In addition, the structural relationships of sPP with other materials (*e.g.*, through epitaxy with oligophenyls, polyethylene, and isotactic polypropylene) have also recently been examined,[14–16] as have the crystallization kinetics of various sPP fractions.[10] However, a detailed study of the morphology of fully syndiotactic polypropylene is still lacking. We had performed such a study earlier[14] with Ziegler–Natta-polymerized sPP, which, as we showed, contained large amounts of isotactic admixtures; these crystallize independently or epitaxially on the syndiotactic crystals, thus both obscuring and modifying their inherent morphologies. We have now performed a morphological investigation on fully syndiotactic samples and attempted to explain the effects of the intermolecular structural disorder on crystallization and morphology and to discuss how these will affect the resulting thermal and mechanical properties of this polymer.

Experimental Section

The materials used in this study were the same as those employed in our most recent investigations,[6,15] *i.e.*, metallocene-polymerized sPP from Himont Co. (courtesy of Dr. T. Simonazzi) with racemic-diad contents of >99%. Thin films of the polymer were deposited from a hot solution in *p*-xylene onto freshly cleaved mica substrates and crystallized under dry N_2 at the desired temperatures for specified durations after evaporation of the solvent and melting of the polymer. The films were then prepared for electron microscopy and diffraction at 100 kV in the manner described earlier.[6,14] Some of the films had been decorated with evaporated polyethylene to delineate the structure of the top surfaces of the lamellar crystals, as reported by Wittmann and Lotz.[17] Thicker films for X-ray diffraction analysis were prepared by compression molding and controlled crystallization. They were then scanned diffractometrically at 2 °C/min in the reflection mode using Ni-filtered Cu Kα radiation while being held at specified temperatures during heating and cooling. Thermal transitions were detected by differential scanning calorimetry at 10 °C/min.

Results and Discussion

Crystallization of sPP in thin films at high temperatures yields large macroscopic single crystals even from the melt.

[†] AT&T Bell Laboratories.

[‡] Institut Charles Sadron.

[⊗] Abstract published in *Advance ACS Abstracts,* September 1, 1994.

0024-9297/94/2227-6603$04.50/0

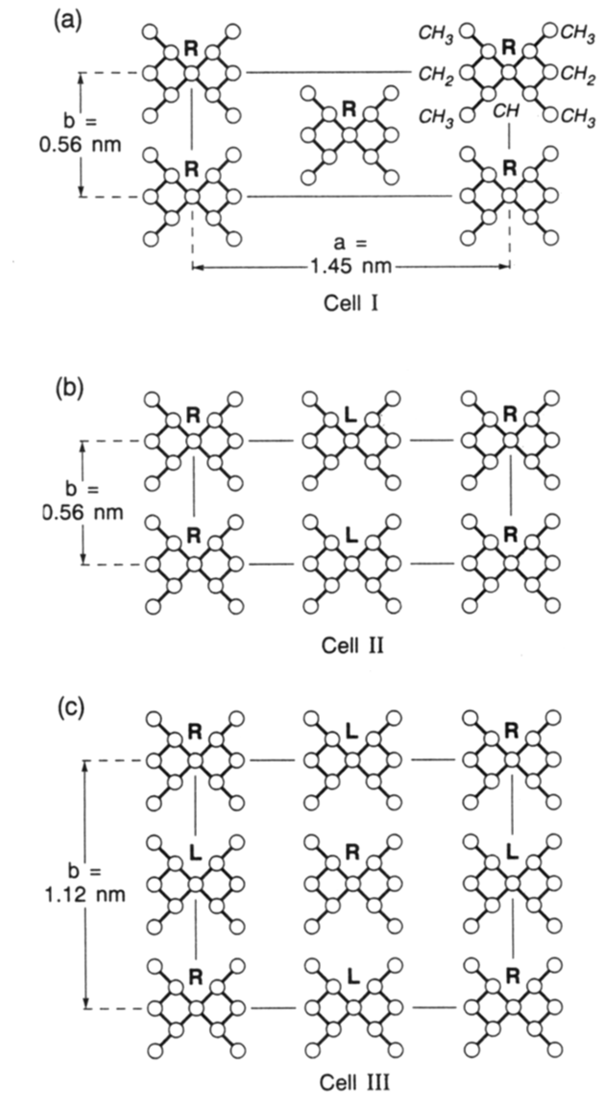

Figure 1. The three proposed unit cells for sPP, shown in projection along the molecular direction (*c*-axis). *R* and *L* signify right- and left-handed helices, respectively.

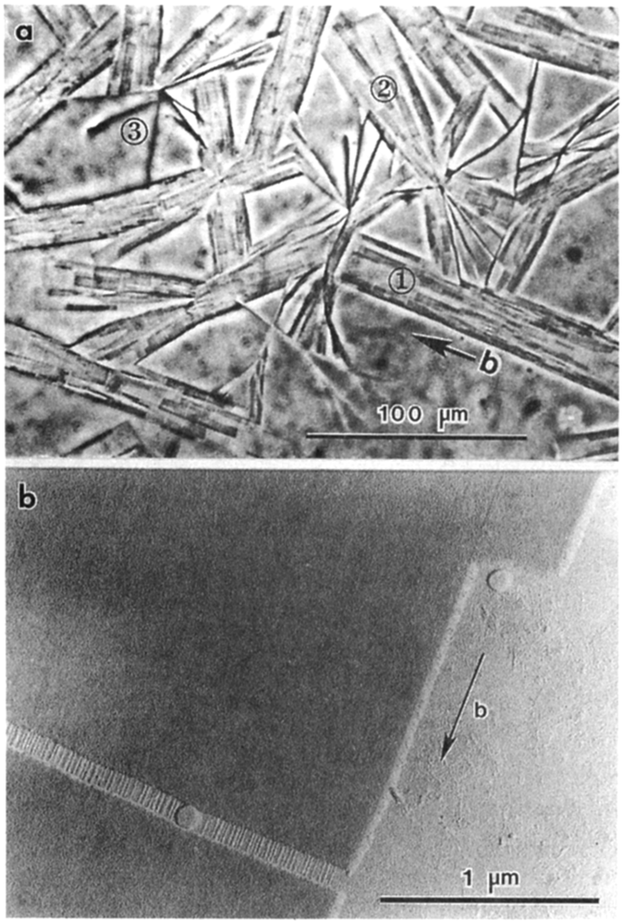

Figure 2. (a) Phase-contrast optical micrograph depicting the overall morphology of sPP crystallized at the highest temperatures (in this case 145 °C for 42 h). Part b shows transmission-electron-micrographic detail from a single crystal in part a exhibiting transverse fracture with fibrillar molecular links.

This is seen in Figure 2a, recorded in phase contrast from a specimen that had been growing at 145 °C for almost 2 days. At optical-microscope magnifications, the morphology consists of three types of feature: (1) very large rectangular single crystals, whose length can exceed 100 μm; (2) crystalline aggregates, which originate from a central point and fan out in typical axialitic fashion; and (3) rodlike crystals, which are simply lamellar stacks on edge, *i.e.* molecules of which have nucleated parallel to the substrate. Examples of these are identified in Figure 2a. Similar structures had also been obtained in our Ziegler–Natta-polymerized sPP (having *ca.* 77% racemic triads), but at *ca.* 35–40 °C lower temperatures and with less regularly defined growth features.[14]

Details of the crystal morphology at this very high growth temperature are seen in the transmission electron micrograph (TEM) of Figure 2b. The sPP lamella is rectangular with a thickness of *ca.* 20 nm and a remarkably smooth and regular faceting. From electron diffraction, the preferred growth direction has been identified as the *b*-axis of the unit cell, so that the growth front corresponds to the (020) planes and the lateral boundaries to the (200) planes. We should notice that the top layer of the lamella appears smooth but with very fine and faint striations parallel to the (200) planes; this feature may be related to the structure of the amorphous surfaces and to the type of chain folding prevalent in these regions, as discussed in detail later in this report. We should also note that the stacks of small edge-on crystals, which were so prevalent at the sides or tops of the previous, less syndioregular sPP lamellae,[14] are absent here; this supports their identification with *isotactic* polypropylene (iPP) molecular segments in syndiodefective specimens.[14] In addition, a large transverse crack is observed in this crystal, which is remarkable in sharpness and linearity over a length exceeding 1 μm. Moreover, fibrils are seen to bridge the two edges of the crack in a taut, extended orientation parallel to the growth direction. These features imply that the transverse crack originated as a result of cleavage of the lamella after its original crystallization and that the fibrils correspond to groups of molecules that had been pulled out during fracture. Of course, fracture could cause not only unfolding of the molecules but also chain cleavage (examples of the latter are given later).

This fracture turns out to be a most typical characteristic of highly syndiotactic polypropylene; we did not observe it in the low-syndiotacticity samples investigated previously.[14] Evidence for profuse incidence of these transverse cracks is presented in Figure 3 (parts a and b) for crystals grown at very high temperatures (142 °C). The cracks are seen here to extend fully across lamellae even when their widths are as large as 10 μm! In so doing, they appear to traverse different sectors and to involve *overlying* lamellae, as well. However, when a crack is initiated on a lamellar overgrowth, it is seen most frequently to be restricted to it and not to cause cleavage of the underlying crystal. Another feature of importance is that cleavage must as a rule be initiated at the *sides* of the crystal: in almost all

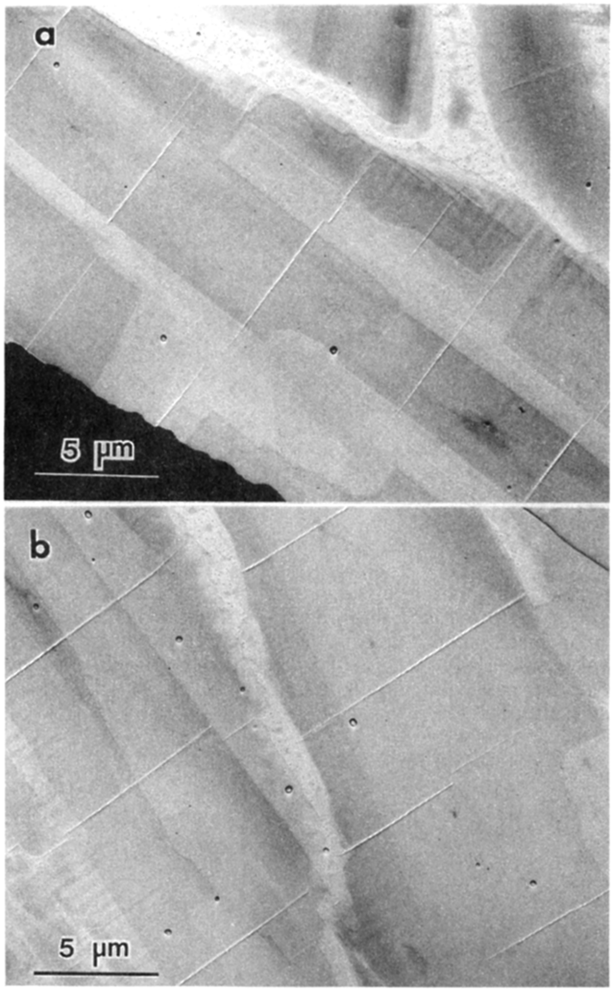

Figure 3. Typical morphologies of sPP lamellae crystallized at 142 °C for 1 day, showing the quasi-periodic transverse lamellar cracks that characterize this polymer.

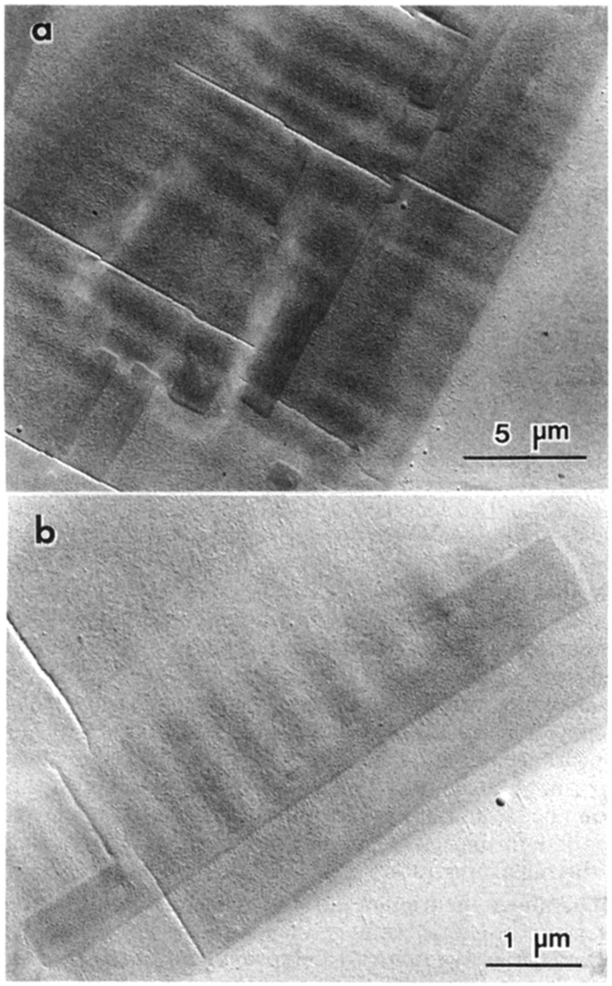

Figure 4. Transmission electron micrographs demonstrating the transverse ripples in sPP crystals grown at very high temperatures (in this case 142 °C for 1 day) and their association with the transverse cracks.

cases the cracks have one or both of their ends at the lamellar edges, and in fact we have never observed a crack that is unequivocally buried within a lamella (cases where that may appear to be so usually involve initiation at overgrowths or screw dislocations). A further feature of great importance relating to these cracks is their quasi-periodicity: as seen in Figure 3, the primary cracks (*i.e.*, those that clearly involve the underlying lamellae and not just the overgrowths) appear on average to occur every 5–7 μm. This quasi-periodicity is consistent for crystals over the entire sample and is not very sensitive to crystallization temperature. Therefore, all these features together suggest that the cracks are initiated as a result of buildup of stresses beyond a certain critical value and that these stresses are not specific to the local growth environment of individual lamellae, but may in fact be an inherent characteristic of this polymer itself. Suggested origins of these stresses are discussed at the end of our report, following full morphological examination and provision of additional structural and thermal evidence.

Another exceptional characteristic of syndiotactic polypropylene crystals is the existence of transverse ripples or undulations that are frequently detectable at the lateral lamellar edges. These are seen almost always in association with the aforementioned cracks. A number of examples is observed in Figure 4 (parts a and b). Because of their smoothness, these ripples are generally difficult to visualize, especially in the case of monolayers. The contrast that we detect in Figure 4 and others is attributable mostly to the effects of shadowing rather than to thickness; this is evidenced by the nonsymmetric distribution of intensity about the midline of each undulation. The shape of the ripples appears generally sinusoidal: the amplitude seems to be fairly uniform (although its value cannot be determined from shadow lengths because of the smoothness of the profile), but most remarkably, their period is *not*. This may be seen by comparison of Figure 4, parts a and b: in the first, typical periodicities are *ca.* 1.0–1.5 μm, while in the second they are generally less than half of that. Moreover, Figure 4b demonstrates that there is a systematic attenuation of the periodicity with distance from the crack. This suggests an association between fracture and ripple formation, with an attendant dampening of the effect at increasing distance from the fracture line. This rationale has been explored semiquantitatively by Tsukruk and Reneker[11] in a very recent attempt to explain our findings on the basis of elastic deformation of thin crystals beyond a critical stress.

Additional information about this very unusual morphological feature can be obtained by low-magnification dark-field TEM, as in Figure 5. The low magnification is deliberately employed in order to record the full width of these very broad lamellae, thus probing the response of different sectors. The dark-field image was constructed from the 020 reflection, since the (0*k*0) planes are parallel to the width of the crystal and, therefore, will highlight strongly any systematic departures from planarity (and thus from the reflecting condition). It is seen in this figure that the waviness is concentrated at the edges of the rectangular lamellae, specifically within the (200) sectors.

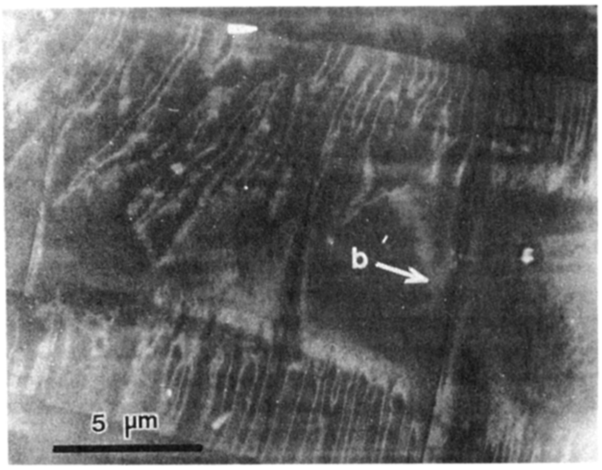

Figure 5. Dark-field (020) electron micrograph of an sPP crystal grown at 140 °C, demonstrating the localization of the transverse ripples within the (200) sectors.

Whether this is associated with the chain folding scheme in the (020) *vs* the (200) sectors is not certain; a possible connection is discussed at the end of this report. Buckling and rippling may also be promoted in thicker, multilayer areas (which proliferate in the (200) sectors through the agency of screw dislocations). This is supported by the appearance of Figure 4b, where the undulations are most prominent in the region of multilamellar overlap. If this rationale is valid, it has clear implications on the relative ease of deformation of lamellae in contact with each other *vs* the mica substrate.

The above-mentioned issue of molecular folding and the structure of the amorphous surfaces are especially important in syndiotactic polypropylene because of its rectangular habit. Thus, in contrast to most other polymers for which the molecules accrete onto crystal substrates that are inclined to the spherulitic growth direction (as, *e.g.*, the {110} in polyethylene), here the largest crystal surfaces by far are the *lateral* ones, which are *parallel* to the growth direction (as, *e.g.*, in α-isotactic polypropylene). In our sPP samples the lateral (200) sectors always appear somewhat thicker and better defined than the (020) growth fronts. This is in agreement with our understanding of the intermolecular packing in sPP,[6] which we have shown to contain $b/4$ defects that frequently involve point vacancies (in molecular-axis projection). As we show schematically in Figure 6, (200) sectors are less affected by these vacancies since they are of molecular dimensions along a, but the growth fronts will reflect the fact that these vacancies correspond to one-half the molecular width along b.

A powerful means to probe the surface structure of polymeric lamellae is by evaporation of polyethylene (PE).[17] The low-molecular-weight fragments deposit in such a way that their molecules are aligned by the local chain topography of the amorphous surfaces of the underlying lamellae. Thus, very immature crystallites "decorate" these lamellae and can be used as markers of the local amorphous structure. This is seen in Figure 7 for two different areas near the (200) lateral edges of sPP lamellae grown at 140 °C. A random orientation of long PE crystallites is seen beyond the edge of the sPP lamellae; however, *on top* of these the PE overgrowths are observed to be much shorter, straighter, and oriented preferentially along the *transverse* direction of the sPP lamellae. This preferred supramolecular orientation may not at first be so obvious from the bright-field images of Figure 7, but it becomes compelling when the Fourier transform of these images is examined. This is obtained using laser-light scattering from the photographic images themselves and is inserted in Figure 7 in the correct orientation. The localization of intensity along the growth direction of the sPP lamellae is clearly demonstrated by these patterns.

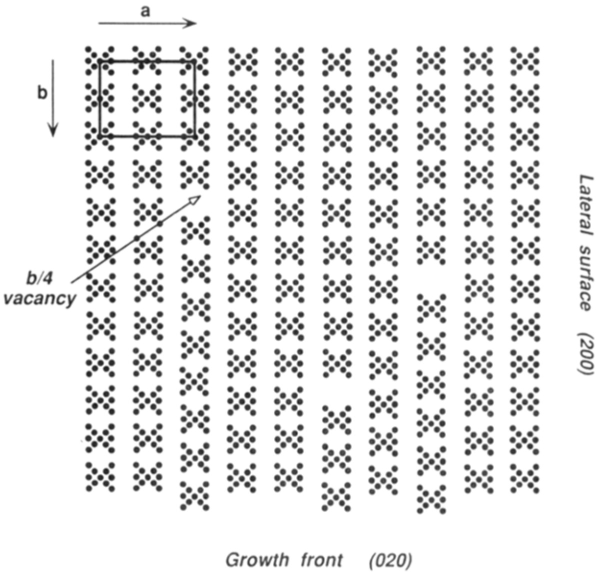

Figure 6. Schematic projection of an sPP crystallite along the c-axis (chain direction), showing the $b/4$ vacancies associated with isochiral packing defects. Note that these vacancies can travel within their own (200) planes and be annihilated by appropriate molecular motions of the adjacent chains within these same (200) planes.

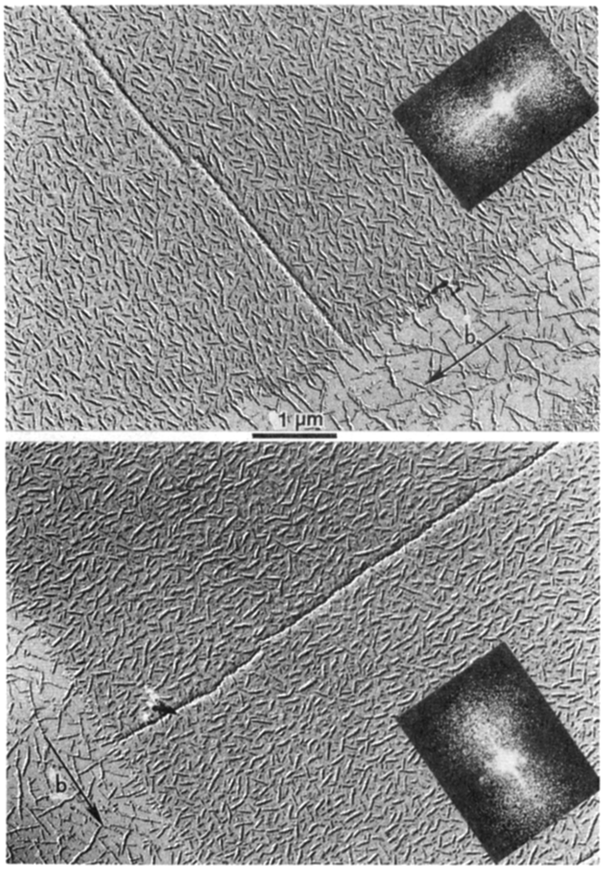

Figure 7. Two examples of polyethylene decoration of the amorphous top surfaces of sPP single crystals grown at 140 °C and exhibiting transverse cracks. The evaporated polyethylene crystallites assume preferred orientations dictated by the fold geometry of the underlying sPP lamellae and evidenced by the light-scattering patterns (insert to each micrograph in correct orientation to the respective fields).

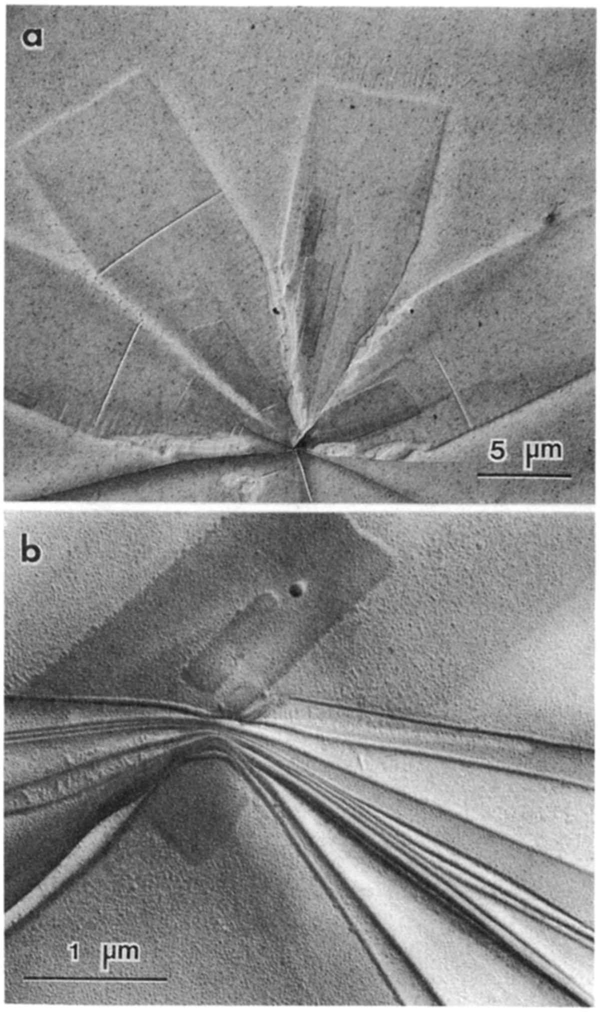

Figure 8. (a) Typical sPP morphology prevailing at a crystallization temperature of 138 °C and consisting of axialites with flat-on and edge-on lamellae. (b) Detail of the nucleus of one such axialite showing splaying and divergence of edge-on lamellae.

The fact that the PE crystallites are oriented transversely to the underlying sPP lamella proves that its amorphous surfaces contain folds or loops that are disposed preferentially *parallel* to the long axis of the crystals. We have deliberately included cracks in the sPP lamellae chosen for reproduction in Figure 7 to probe additionally the *localized* orientation at the crack boundaries. As seen in this figure, this orientation is not different from the overall one, proving that a hypothetical change in the chain-folding scheme (*e.g.* from longitudinal to transverse) is not at the root of this fracture. Its origins must therefore be related more to the crystalline, rather than the amorphous, layer of the sPP lamellae, which lends further support to our argument relating the $b/4$ defects and associated half-molecular-width vacancies to initiation of these cracks. In contrast to the very regular folding demonstrated for the (200) sectors, their (020) couterparts, which are longitudinally disposed along the growth direction, yielded much more random PE decoration on their surfaces. This is again consistent with the greater effect of the $b/4$ defects on the growth planes *vs* the lateral lamellar surfaces.

Having examined in detail the morphology of sPP single crystals grown at the highest temperatures, we now report on crystallization and morphology at progressively lower temperatures. Typical structures obtained at 138 °C are seen in Figure 8. These are generally axialitic (Figure 8a), originate from central nuclei, and fan out rapidly to yield multilayer aggregates of rectangular laths. Nucleation is not common on impurities, but rather self-nucleation takes place on favorably disposed molecular stems. Frequently, these are parallel to the substrate (and thus possibly initiated on atomic steps of the mica), leading to fibrous-appearing edge-on lamellae. An example of this is given (at higher magnification) in Figure 8b, in which successive layers of edge-on crystals that splay apart as they grow out are clearly seen.

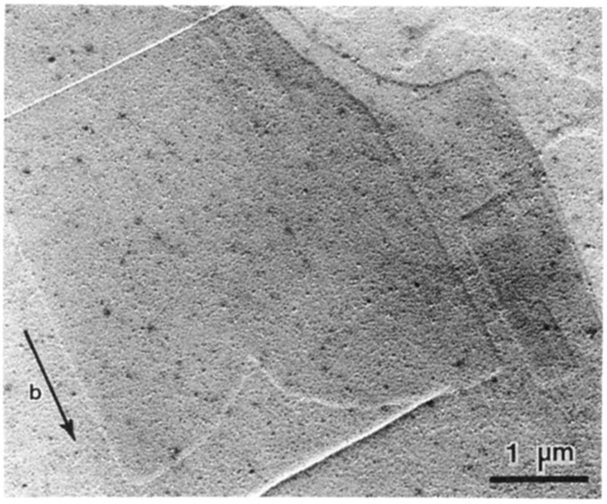

Figure 9. An example of an sPP lamella grown at 138 °C showing regular (200) lateral facets with irregular infilling of the (020) growth sector from the sides.

The sectoring of the sPP lamellae is also visible in Figure 8a; the (200) sectors appear slightly darker than the (020) sectors, which indicates increased thickness (and occasionally additional layers). In the region near the nucleus, where the adjacent lamellae impinge, their serrated oblique edges consist of extensive (020)/(200) microfaceting. Once again the (020) growth fronts appear somewhat less regularly defined than the (200) lateral sides. In fact, at this temperature we have observed a number of instances in which the lateral edges appear to have formed first and the remaining part of the crystal to have lagged behind and to have "filled in" from the sides. A striking example of this is seen in Figure 9. Such instances become more common with decreasing crystallization temperature, but are also more difficult to detect because of rapid growth and extensive impingement of lamellae.

Another phenomenon that we have been able to detect at this lower crystallization temperature is twinning. In fact, twinning is exceedingly rare in sPP. We attribute this to a combination of reasons involving the shape and symmetry of the molecules, as well as their orientation in the unit cell. As seen in Figure 6, the chains have a rectangular cross section whose sides and major symmetry axes are all parallel to the unit-cell axes. As a result, oblique twin planes are not favored in sPP, in contrast, for example, to polyethylene whose molecules have a more isometric envelope with all-trans planes that are inclined (in projection) to the unit-cell axes. The clearest case of twinning that we have observed in sPP is seen in Figure 10a; a higher magnification of the central region of the twinned lamellae is given in Figure 10b. The two intersecting crystals have been directly nucleated in a twin mode and have grown with their respective b-axes 52° apart. There exists no reasonable twin plane at 26° from the b-direction (the closest low-index plane is the (310) at 23°, but this is not at all a well-populated plane). On the other hand, 52° corresponds to the angle between the (200) and the (220) planes, which are the two most densely populated sets of crystallographic planes in sPP. This strongly suggests the possibility that the observed twin is actually a *rotation* twin, with the b-axis of the second

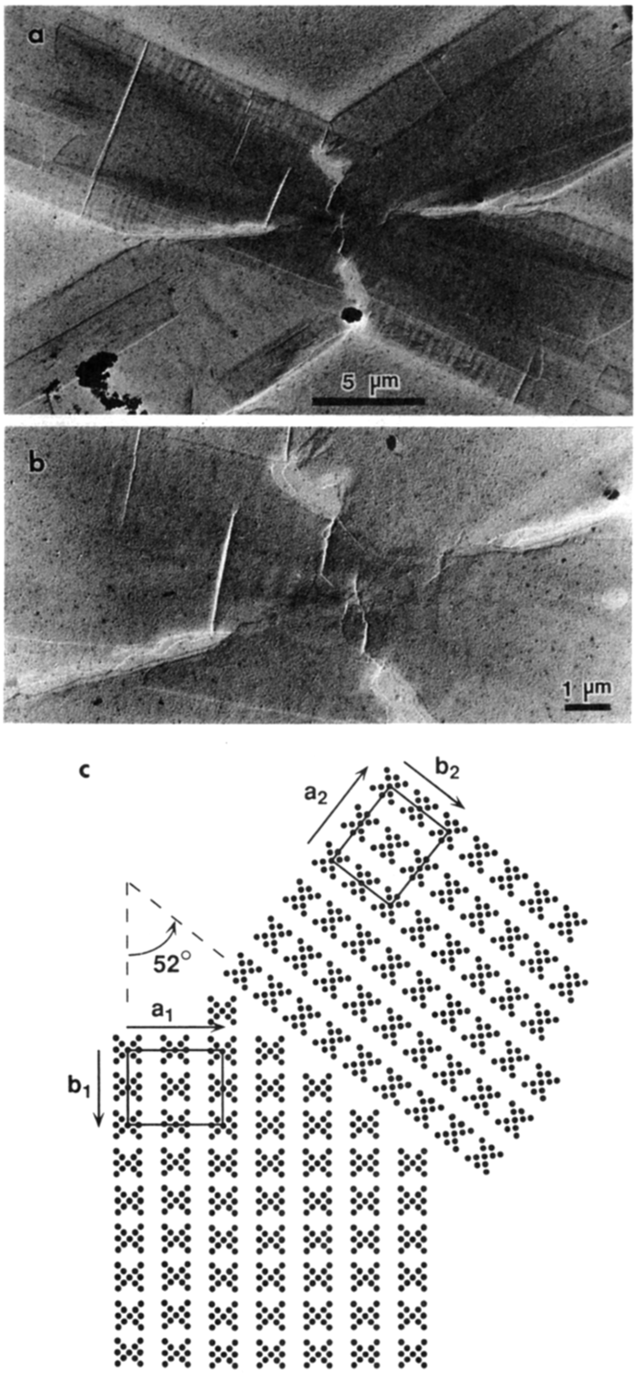

Figure 10. (a) An incidence of rotation twinning in sPP crystals (this sample grown at 138 °C). (b) Detail of the central region of part a showing initiation of the twinned growth. (c) Schematic lattice orientation consistent with the rotation twinning of parts a and b and involving matching of the (200) and (110) planes of the respective crystals.

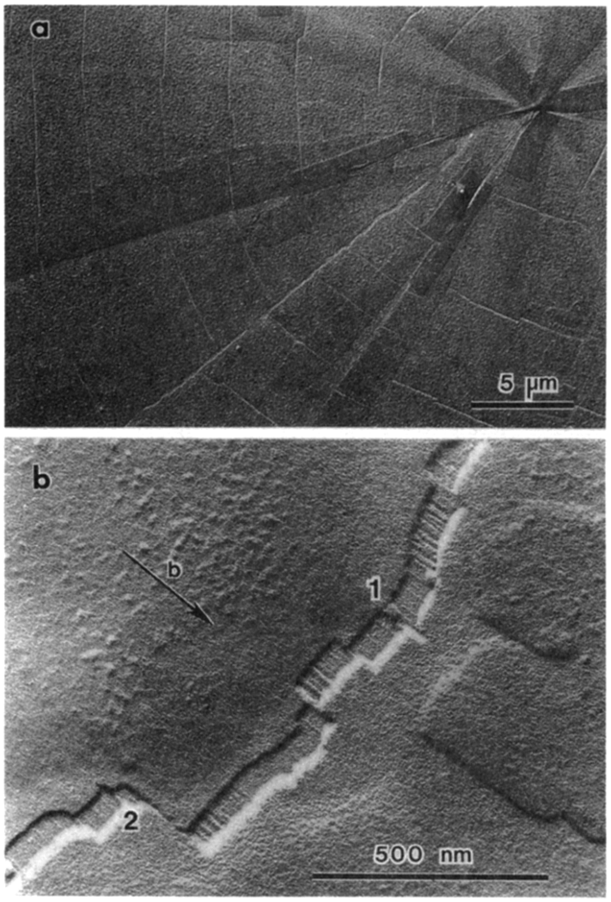

Figure 11. (a) Typical morphology of sPP-crystalline aggregates grown at 130 °C. Quasi-periodic transverse fractures are seen in tangential orientation. (b) High-magnification detail showing slippage of (200) planes with cleavage of the (020). Minute mosaic blocks that are pulled out coherently are identified as "1" and "2".

crystal superposed onto the [110] direction of the first. The corresponding lattice relationship would be as shown schematically in Figure 10c, which appears sterically quite reasonable. This is also facilitated by the fact that four molecules in *b*-axis packing can be very closely accommodated in the space of three chains along [110]; the actual distance ratio is 92%. The small vacancies that are produced at the composition plane are in reality quite similar to the *b*/4 vacancies that commonly exist in sPP crystals (compare Figures 10 and 6). The above interpretations explain why twinning is so rare in sPP and why when manifested it does so in the form of rotation twinning with twin axis parallel to the molecular direction. Rotation twinning is in turn very rare among other polymers, being best known for isotactic polypropylene,[18] where, however, the twin axis is at an angle to the chain axis).

Lowering the crystallization temperature further leads to the morphology seen in Figure 11a. At 130 °C full spherulites are obtained, at least in the sense of growing radially outwards from central nuclei in all directions. Nevertheless, the lamellae are preferentially parallel to the substrate and, more importantly, they fan out to yield essentially single-crystalline sectors. These are clearly seen in Figure 11a, together with the by now familiar cracks, which are now arranged tangentially and which extend throughout the widths of the diverging lamellae. As before, they exhibit a quasi-periodic spacing, which is now somewhat tighter, *i.e. ca.* 3–6 μm. One difference is that at this lower crystallization temperature the cracks are no longer straight over large distances but are extensively microfaceted on a very fine scale. From the evidence of Figure 11b, there is no doubt that there is facile slippage of the (200) planes, which are nearly always straight at the cracks, versus fracture on the transverse direction, which is generally curved or irregular. This lends further support to our proposed localized folding *along* the lamellar growth direction [010]. It is remarkable to realize from this figure the small size of mosaic-like blocks that are pulled out coherently during fracture (*i.e.* without undergoing yield and fibrillation): the two smallest ones in Figure 11b are numbered "1" and "2" and correspond to widths of only 17 and 6 nm, (*i.e.*, 23 and 8 molecules!), respectively.

Our final morphological results are for samples crystallized at much lower temperatures, *i.e.* 120 and 100 °C (Figure 12). Despite the very rapid growth at these high

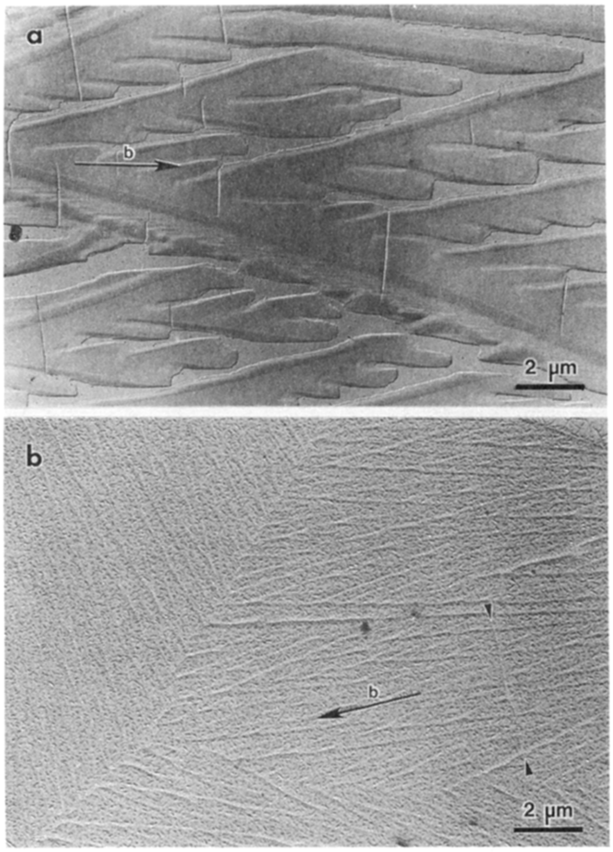

Figure 12. (a) Typical morphology of sPP crystallized at 120 °C. A crystallographically branched dendritic superstructure of lamellae with rounded (200) and (020) facets is seen growing along the *b*-axis. Quasi-periodic fractures are again visible normal to that direction. (b) Morphology of sPP spherulites grown at 100 °C and exhibiting profuse branching. A transverse crack is identified with arrowheads.

undercoolings, the crystals are still platelike, but much more irregular. Their underlying rectangular habit is still recognizable at 120 °C (Figure 12a), but with distinctly rounded (200) and (020) facets. The overall growth is now dominated by profuse *dendritic* branching. Electron diffraction from such areas confirms their generally uniform unit-cell orientation and crystallographic branching. We should again note the absence of small edge-on lamellae at the lateral (200) sides of the sPP crystals, confirming our previous[14] association of these with iPP admixtures in lower syndiotacticity specimens. Moreover, despite rapid spherulitic crystallization at 120 °C, transverse cracks are still in evidence with similar spacings and lengths as before. It is only at crystallization temperatures of *ca.* 100 °C, where more typically spherulitic morphologies now prevail, that cracks become sparse (one case is identified in Figure 12b). These findings demonstrate that crystal fracture in sPP is not a phenomenon restricted to fairly perfect lattices grown slowly at high temperatures. Its origins must therefore be sought in terms of the anisotropic thermal properties of the sPP crystals.

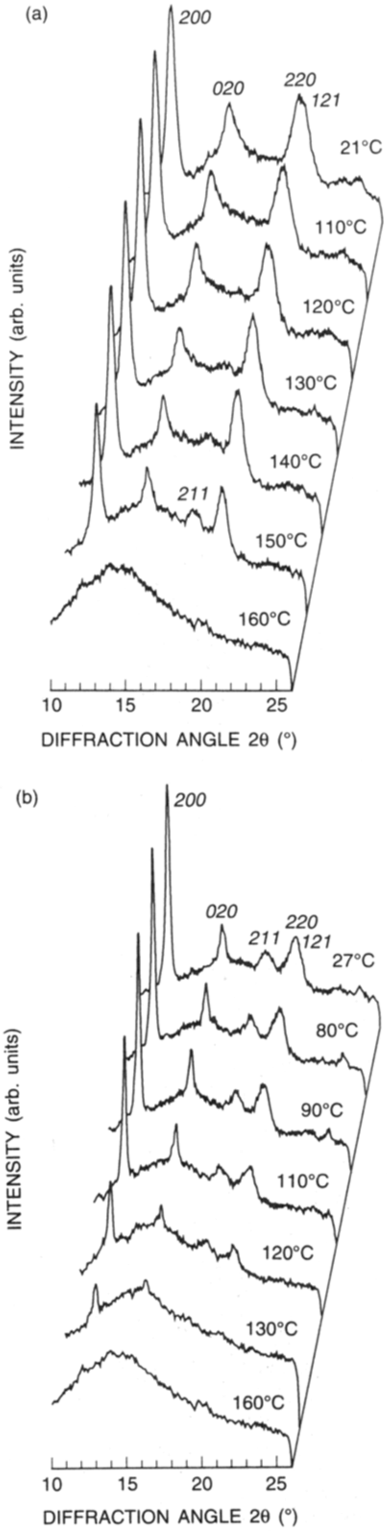

Figure 13. Successive X-ray diffractograms of sPP that had been quenched to ambient (a) during heating to the melting point and (b) during subsequent cooling.

For this reason we examined the X-ray diffractograms of this polymer during a heating and cooling cycle between ambient temperature and the melting point; these are shown in Figure 13. The initial pattern at 21 °C comes from a specimen that had been rapidly quenched from the melt and indicates the expected[3,6] substantial packing disorder along *b* (as evidenced by the breadth of the peaks and the absence of the 211 reflection). However, a remarkable crystallographic transformation is evidenced during heating: from *ca.* 120 °C upward, an additional peak in the vicinity of 18° 2θ is seen to be growing, while at the same time the other reflections are being narrowed. As we demonstrated recently,[6] this new peak corresponds to the 211 reflection, which is the primary reflection identifying the new doubled unit cell (cell III) *and is thus the hallmark of fully antichiral packing*. Its appearance during heating proves that the molecular chains in the crystal undergo an extensive reorganization above *ca.* 120 °C by repacking in an antichiral manner. This requires substantial motion within the crystal lattice, specifically the *b*-axis, which is the one within which the chirality-

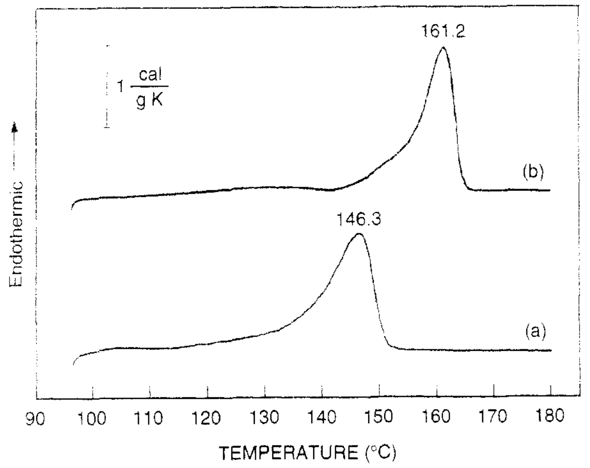

Figure 14. DSC thermograms of sPP: (a) sample originally quenched to ambient and (b) sample crystallized at 140 °C.

associated $b/4$ packing defects are localized (see again Figure 6). It should thus not be surprising that thermal motions predominate in the growth direction and could therefore contribute critically to the generation of the observed transverse cracks. Moreover, the transport of the $b/4$ vacancies along the b-direction might also cause occasional localization of such defects adjacently to each other. These would be primary candidates for the locus of initiation of the transverse cracks. We should also notice from Figure 13b that, in contrast to the quenched specimen, a sample slowly cooled from the melt shows the 211 reflection directly upon crystallization; this reflection is seen to grow together with all the others in Figure 13b, as greater crystallinity is attained at lower temperatures. Thus, such a specimen is not expected to show significant additional solid-state recrystallization toward cell III during subsequent reheating.

These characteristics of the heating-induced solid-state transformation toward a fully antichiral packing are also reflected in the DSC thermograms of syndiotactic polypropylene (see Figure 14). The original, defectively packed, quenched specimen gives curve a, which exhibits a very broad endotherm that begins well below 120 °C. There is no exact correspondence between the melting temperatures in the DSC and X-ray experiments because of the different heating programs. Nevertheless, it is clear that for specimens isothermally crystallized at 140 °C (curve b), which we know from our electron-diffraction study[6] to be almost fully in the regularly antichiral cell III, not only is the melting peak *ca.* 15 °C higher and much narrower but there are no indications of an endothermic process below *ca.* 145 °C. This suggests that at least a major part of the breadth at lower temperatures in the original specimen reflects the recrystallization to regularly antichiral packing (cell III).

From the diffractograms of Figure 13a,b, we can extract the unit-cell dimensions as functions of temperature during heating and cooling. The variation of the a- and b-axes is given in Figure 15. The actual linear thermal expansion coefficients from this figure are 2.02×10^{-5} nm/°C along a and 1.826×10^{-4} nm/°C along b, or (as fractions of unit-cell lengths) 1.393×10^{-5}/°C and 1.630×10^{-4}/°C, respectively. This order-of-magnitude greater expansion (and contraction) along the preferred growth direction of sPP crystals is remarkable and is undoubtedly at the root of their extraordinary transverse fracture and rippling described in this report.

Coupled with the mobility of point vacancies and molecular stems along the b direction, these highly anisotropic interchain thermal properties are expected to have a profound (and *negative*) effect on the mechanical properties of sPP crystals. The ripples and fractures that are introduced transversely during cooling as a result of an order-of-magnitude greater contraction longitudinally will undoubtedly cause mechanical weakening of bulk specimens of this polymer to a potentially serious extent. The same will be true for the recrystallization into the preferred antichiral packing if specimens are reheated (*e.g.* annealed) after industrial melt-forming operations (*e.g.* extrusion, molding) that involve rapid cooling.

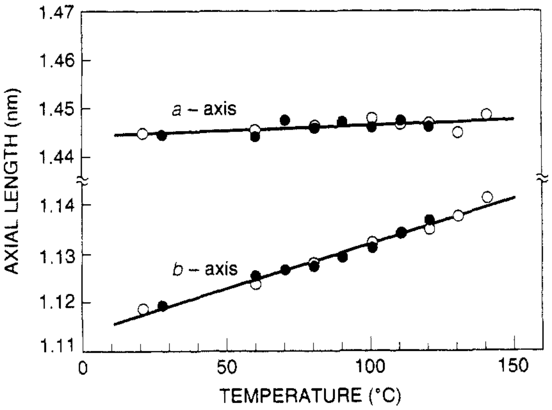

Figure 15. Thermal expansion and contraction of the unit cell of sPP along the a- and b-axes. ○, heating; ●, cooling.

We may enquire as to how unusual the phenomenon of anisotropic fracturing and rippling might be among crystalline polymers. While cracks are occasionally seen in some such materials, and anisotropies in intermolecular thermal expansion are well-known (*e.g.* in polyethylene or poly(p-phenylene sulfide)), such extensive, regular, and fairly periodic fracturing is not observed. This may be due to the additional characteristics of sPP crystal lattices involving large intermolecular motions in one direction (normal to the chain and along the growth axes), as well as potential aggregation of vacancies. The one example bearing strong similarity to sPP in terms of both fracture and rippling is the case of polydiacetylene. In 1989 we showed similar cracks in optical and electron micrographs of one such polydiacetylene, as well as electron-diffraction patterns from single crystals indicating a very similar packing disorder as in sPP (evident through streaking of $01l$ reflections normal to the molecular axis).[19] Similar optical findings of cracks and a preliminary elastic energy calculation were also presented by Berrêhar *et al.*,[20] who in subsequent work[21] analyzed these in detail on the basis of the Grinfeld instability.[22] At that time, they also presented evidence for "wrinkles" having the same orientation as the cracks and interpreted the latter as arising at points of stress concentration within the wrinkles (with the stress associated with the solid-state polymerization of the diacetylene single crystals).[21] Tsukruk and Reneker[11] are in the process of adapting these findings from polydiacetylene to the case of syndiotactic polypropylene.

In discussing possible origins of these ripples, we should underline our finding that these form preferentially in the lateral (200) sectors where folds are parallel to the maximal thermal contraction of the crystal lattice. This observation raises the issue of differential thermal contraction of the fold surface in relation to that of the crystal lattice. We assume that the fold surface (consisting of folds and longer loops oriented in a more-or-less parallel fashion) behaves similarly to a stretched amorphous bulk material with anchoring points on the crystalline core that serve a similar function as physical or chemical cross-links in the bulk. This assumption appears reasonable in light of the findings of Fischer and Kloos[23] on the similarity of the glass transition of fold surfaces and bulk amorphous material. In such a material the thermal expansion coefficient along the chain axis is nearly zero (or even slightly negative). Therefore, the major part of the overall volumetric thermal expansion is ascribable to the linear expansion normal to the chain axes. In (020) sectors of sPP, which exhibit no ripples, the transverse fold orientation parallel to the *a*-axis results in essential matching of the low thermal expansion coefficients of the amorphous and crystalline parts. In the *b*-axis direction of these same (020) sectors, amorphous and crystalline layers have comparable expansion coefficients of the order of 10^{-4}. As a result, contraction of the fold surface can accommodate that of the crystalline core upon cooling. This situation is completely reversed in the (200) sectors: upon cooling, the very large contraction of the crystalline core along *b* is opposed by zero contraction (or even slight expansion) of the fold surface. As a result, the (200) sectors may thus be unable to contract macroscopically on cooling to the extent experienced by their (020) counterparts, so that they deform by developing ripples. In this manner, formation of exceptionally large rectangular crystals on a flat substrate (through thin-film growth), coupled with the unusually high difference in thermal expansion along their two directions, highlights the structural consequences of thermal stresses in polymer crystals.

Conclusions

Syndiotactic polypropylene crystals grown from the melt possess a rectangular habit with long and short sides parallel to the *b*- and *a*-axes of the unit cell, respectively. The rectangular habit *per se* provides a direct morphological verification of our proposed unit cells (III and II), since cell I would require inclined {110} facets, which are never seen. The lateral (200) facets are much more regular than the (020) growth face, which in some cases appears crenelated and infilled from the two lateral sides. This is consistent with the localization and motion of *b*/4 vacancies within individual (200) planes, specifically at boundaries between the dominant antichiral packing and the occasional isochiral defects. At lower crystallization temperatures (*e.g.* 120 °C) the growth and lateral facets become rounded and the overall crystallization becomes dendritic. However, at no temperature did we detect the stacks of edge-on lamellae that we had reported earlier in a sample of *ca.* 77% syndiotacticity, supporting our previous identification of these with isotactic polypropylene admixtures arising from the less syndiospecific Ziegler–Natta catalysts. The increased regularity in the (200) sectors extends also to their folding, which we showed through decoration with evaporated polyethylene to be oriented overwhelmingly along the *b*-axis.

The most novel and important characteristic of syndiotactic polypropylene morphology discovered in our study is the formation of transverse cracks in its crystals grown at high temperatures (generally from 145 down to *ca.* 100 °C). These cracks frequently extend over many micrometers throughout the entire width of individual lamellae and their overgrowths. They are quasi-periodic at *ca.* 3–7 μm and are frequently accompanied in the (200) sectors with transverse bands of undulations or ripples having variable periodicities that are generally a fraction of 1 μm. The fractures are crystallographically sharp in the (020) planes, are accompanied by slippage between (200) planes, and are commonly bridged by fibrils. We explained these phenomena on the basis of an approximate order-of-magnitude higher thermal expansion coefficient between (020) planes than between their (200) counterparts. This may be related to the motion of packing defects and vacancies in the *b*-direction; aggregation of such *b*/4 vacancies may be involved in nucleating fracture. Moreover, we showed that heating of quenched specimens above *ca.* 120 °C causes a reorganization in chain packing toward the fully antichiral cell III. We believe that these large-scale molecular motions in the *b*-direction and the associated transverse fractures and ripples will have severe negative consequences on the mechanical properties of syndiotactic polypropylene.

Acknowledgment. We are grateful to Dr. T. Simonazzi of Himont Co. for his kind provision of an experimental sPP sample.

References and Notes

(1) Natta, G.; Pasquon, I.; Corradini, P.; Peraldo, M.; Pegoraro, M.; Zambelli, A. *Rend. Acd. Naz. Lincei* **1960**, *28*, 539.
(2) Corradini, P.; Natta, G.; Ganis, P.; Temussi, P. A. *J. Polym. Sci., Part C* **1967**, *16*, 2477.
(3) Lotz, B.; Lovinger, A. J.; Cais, R. E. *Macromolecules* **1988**, *21*, 2375.
(4) Lovinger, A. J.; Lotz, B.; Davis, D. D. *Polymer* **1990**, *31*, 2253.
(5) Ewen, J. A.; Jones, R. L.; Razavi, A.; Ferrara, J. D. *J. Am. Chem. Soc.* **1988**, *110*, 6255.
(6) Lovinger, A. J.; Lotz, B.; Davis, D. D.; Padden, F. J., Jr. *Macromolecules* **1993**, *26*, 3494.
(7) Auriemma, F.; De Rosa, C.; Corradini, P. *Macromolecules* **1993**, *26*, 5719.
(8) De Rosa, C.; Corradini, P. *Macromolecules* **1993**, *26*, 5711.
(9) Sozzani, P.; Simonutti, R.; Galimberti, M. *Macromolecules* **1993**, *26*, 5782.
(10) Rodriguez-Arnold, J.; Zhang, A.; Cheng, S. Z. D.; Lovinger, A. J.; Hsieh, E. T.; Chu, P.; Johnson, T. W.; Honnell, K. G.; Geerts, R. G.; Palackal, S. J.; Hawley, G. R.; Welch, B. *Polymer* **1994**, *35*, 1884.
(11) Tsukruk, V. V.; Reneker, D. H. *Bull. Am. Phys. Soc.* **1994**, *39*, 714.
(12) Galambos, A. F.; Wolkowicz, M.; Zeigler, R.; Galimberti, M. *Polym. Mater. Sci. Eng.* **1991**, *64*, 45.
(13) Chatani, Y.; Maruyama, H.; Noguchi, K.; Asanuma, T.; Shiomura, T. *J. Polym. Sci., Part C Polym. Lett.* **1990**, *28*, 393.
(14) Lovinger, A. J.; Davis, D. D.; Lotz, B. *Macromolecules* **1991**, *24*, 552.
(15) Stocker, W.; Schumacher, M.; Graff, S.; Lang, J.; Wittmann, J. C.; Lovinger, A. J.; Lotz, B. *Macromolecules*, in press.
(16) Schumacher, M.; Lovinger, A. J.; Agarwal, P.; Wittmann, J. C.; Lotz, B. *Macromolecules*, in press.
(17) Wittmann, J. C.; Lotz, B. *J. Polym. Sci., Polym. Phys. Ed.* **1985**, *23*, 205.
(18) Lotz, B.; Wittmann, J. C. *J. Polym. Sci., Polym. Phys. Ed.* **1986**, *24*, 1541.
(19) Tanaka, H.; Gomez, M. A.; Tonelli, A. E.; Lovinger, A. J.; Davis, D. D. *Macromolecules* **1989**, *22*, 2427.
(20) Berréhar, J.; Lapersonne-Meyer, C.; Schott, M.; Villain, J. *J. Phys. (Paris)* **1989**, *50*, 923.
(21) Berréhar, J.; Caroli, C.; Lapersonne-Meyer, C.; Schott, M. *Phys. Rev. B* **1992**, *46*, 13487.
(22) Grinfeld, M. A. *Sov. Phys. Dokl.* **1986**, *31*, 831.
(23) Fischer, E. W.; Kloos, F. *J. Polym. Sci., Part B Polym. Phys.* **1970**, *8*, 685.